RF Transmission Power Loss Variation with Abdominal Tissues Thicknesses for Ingestible Source

Chee Wee Kim and Terence Shie Ping See
Institute for Infocomm Research, Singapore
Email: [cwkim, spsee]@i2r.a-star.edu.sg

Abstract— **This paper presents the investigation of the variation in RF (radio frequency) transmission power loss at 403 MHz and 923 MHz due to different tissue thicknesses using a layered planar tissue model of skin, subcutaneous fat, abdomen muscle, visceral fat and small intestine. The generalized transmission coefficient is used to calculate the transmission power loss of various tissue thickness combinations that are based on medical findings of human abdomen composition. The calculations show large transmission power loss variations (up to 10 dB). The effect of visceral fat thickness variation is the largest. The results are useful for the design of wireless communications module of an ingestible device, e.g. capsule endoscope.**

Index Terms— **Microwave propagation, biomedical telemetry, numerical phantom**

I. INTRODUCTION

Wireless capsule endoscopy offers a non-invasive method to capture images of the gastro-intestinal (GI) tract for detection and diagnosis of diseases such as obscure GI bleeding, tumors, polyps, celiac and Crohn's disease [1]. Compared to traditional wired endoscopy, it eases the patient from pain, discomfort and the need for sedation, while being able to reach the full length of the small intestine. The capsule is also able to perform biopsy and therapeutic functions [2], [3]. In order for the capsule to perform the additional functions, power management serves an important role [4]. The RF (radio frequency) transmitter is one of the components that consume a significant amount of power. Therefore, a study of the RF propagation from an ingestible source inside the small intestine to an external receiver on the body will be necessary to explore the possibility of reducing the transmit power.

There have been studies of in-to-off body RF propagation. The radiation performance outside the body has been investigated [5]–[6]. The effects of organ contents on the propagation channel were considered [7]. These studies were conducted using numerical human voxel phantoms that are based on specific human subjects. In consideration of the different thicknesses of the tissues, a planar tissue model that comprises of homogeneous layers of skin, fat and muscle was used [8], [9]. However, in this study, the specific absorption rate (SAR) is of primary interest and the RF transmission characteristics have not been analyzed. From the RF channel studies using different numerical human phantoms, it has been shown that the radiation characteristics are subject and source location specific [10].

This paper presents the investigation of the effects of different thicknesses of the body tissues on the transmission power loss variation. A planar model that consists of skin, subcutaneous fat, abdominal muscle, visceral fat and small intestine is adopted. The tissues can be divided into three categories (low, mid and high tertile) according to the visceral fat thickness [11]. The generalized transmission coefficient [12] is then used to obtain the transmission power loss through these layered tissue mediums. The effects of the thicknesses of subcutaneous fat, abdominal muscle and visceral fat are investigated and the range of the power loss for each category is obtained.

The organization of the paper is as follows. Section II covers the tissue composition of the human abdomen. A layered planar model is then used to simplify the representation of these tissues. Section III presents the equations for obtaining the generalized transmission coefficient. Section IV presents the effects of the different thicknesses of the tissues on the RF transmission power loss. Section V covers the discussion of the implications of the results to the design of wireless communications for capsule endoscopy.

II. COMPOSITION OF THE HUMAN ABDOMEN

For wireless capsule endoscopy, the internal source is located in the small intestine while the external receiver is placed close to the human belly. The interior of the human abdomen thus becomes the propagation channel. The tissues that are of interest consist of the small intestine, visceral fat, abdomen muscle, subcutaneous fat and skin. Subcutaneous fat refers to the fat that is found just under the skin while visceral fat refers to the fat that is found in the abdominal cavity and packed in between the organs.

Fig. 1 shows the cross-section of the human abdomen that is obtained from the HUGO phantom [13], where the different compositions of small intestine, visceral fat, abdomen muscle, subcutaneous fat and skin can be observed. In this study, a layered planar model as shown in Fig. 2 will be used to represent the propagation channel inside the body. For the

small intestine region that is furthest from the skin surface, it is followed by a large region of back muscle. As it will be shown later, the effect of the transition from the small intestine to muscle is negligible. Hence, the layered planar model starts with the air region and terminates with the small intestine region.

The frequencies that are commonly used in capsule endoscopy are the MICS (Medical Implant Communication Service) and ISM (Industrial, Scientific and Medical) band. Table I shows the dielectric properties of the tissues at 403 MHz (MICS) and 923 MHz (ISM) [14]. Assuming uniform plane waves, the attenuation per cm through these tissues are obtained and tabulated in Table II. Similarly, the transmission coefficients through the different tissues can be obtained. The percentage of incident power transmitted and the corresponding transmission power loss (in dB) are tabulated in Table III. It can be seen that the small intestine has the largest attenuation, followed by skin, muscle and fat. The RF transmission power loss is greatest from skin to air while there is negligible loss from small intestine to muscle. There is smaller attenuation loss but larger transmission loss for 403 MHz as compared to that for 923 MHz. This indicates that 403 MHz can be more suitable for implant-to-implant communications while 923 MHz is more suitable for in-to-off body communications.

Table IV tabulates the thicknesses of skin, abdominal muscle, subcutaneous and visceral fat for low, middle and high tertile male subjects, where the grouping is based on the visceral fat thickness [11]. In that study, the visceral fat thickness was defined as the distance between the anterior wall of the aorta and the internal face of the rectoabdominal muscle perpendicular to the aorta. The thicknesses for skin and abdominal muscle are obtained from [15] and [16] respectively. These values will be used to investigate the transmission power loss for the layered planar tissue model. For the HUGO model, the thicknesses of the subcutaneous fat, abdominal muscle and visceral fat tissues at the center of the belly are 28 mm, 16 mm and 100 mm, respectively.

Fig. 1. Cross-section of the abdomen region from the HUGO model. (Dark regions−large and small intestines; light grey regions−muscles; lightest regions−fat).

Fig. 2. Layered planar tissue model.

TABLE I
RELATIVE PERMITTIVITY (ε_r) AND CONDUCTIVITY (σ) OF THE TISSUES AT 403 MHZ AND 923 MHZ [14]

Tissue	Property	403 MHz	923 MHz
Skin	ε_r	46.7	41.3
	σ	0.69	0.87
Fat	ε_r	5.58	5.46
	σ	0.04	0.05
Muscle	ε_r	57.1	55.0
	σ	0.80	0.95
Small intestine	ε_r	66.1	59.3
	σ	1.90	2.18

TABLE II
ATTENUATION AT 403 MHZ AND 923 MHZ

Tissue	Attenuation (dB/cm)	
	403 MHz	923 MHz
Skin	2.0338	2.1714
Fat	0.3433	0.3487
Muscle	1.9706	2.0676
Small Intestine	3.8329	4.3863

TABLE III
PERCENTAGE OF INCIDENT POWER TRANSMITTED AND THE TRANSMISSION POWER LOSS FOR VARIOUS MEDIUM TRANSITIONS AT 403 MHZ AND 923 MHZ

Medium transition	% of incident power transmitted		Power loss (dB)	
	403 MHz	923 MHz	403 MHz	923 MHz
Skin and fat	75.79	77.64	1.2039	1.0991
Small intestine and muscle	99.32	99.85	0.0296	0.0065
Muscle and fat	71.28	72.51	1.4703	1.3960
Small intestine and fat	64.92	69.51	1.8762	1.5795
Skin and air	43.76	45.94	3.5892	3.3781

TABLE IV
THICKNESS OF VARIOUS TISSUES FOR LOW, MID AND HIGH TERTILE MALE SUBJECTS*

Tissue	Range of thickness (mm)		
	Low tertile	Mid tertile	High tertile
Skin	1.1 – 1.6	1.1 – 1.6	1.1 – 1.6
Subcutaneous fat	13.5 – 28.5	14.0 – 28.0	11.5 – 28.0
Abdominal muscle	8.0 – 16.0	8.0 – 16.0	8.0 – 16.0
Visceral fat	11.0 – 44.0	44.0 – 57.9	58.0 – 104.0

*groupings into low, mid and high tertiles are according to the visceral fat thickness [11].

III. GENERALIZED TRANSMISSION COEFFICIENT

A planar inhomogeneous half-space with the permeability μ_i, permittivity ε_i and conductivity σ_i varying in different regions is considered as shown in Fig. 3. A uniform plane wave travelling in the $+z$ direction in region i can be represented by:

$$e_{iy} = e_0 e^{-jk_i z}, \tag{1}$$

where $k_i = \omega\sqrt{\mu_i\left(\varepsilon_i - j\frac{\sigma_i}{\omega}\right)}$ is the wavenumber of region i and $\omega = 2\pi f$ is the angular frequency.

If there are only two layers of medium, i.e. the wave travels from region i to region $i+1$ only, the reflection and transmission coefficients are given by:

$$R_{i,i+1} = \frac{\mu_{i+1}k_i - \mu_i k_{i+1}}{\mu_{i+1}k_i + \mu_i k_{i+1}}, \tag{2}$$

$$T_{i,i+1} = \frac{2\mu_{i+1}k_i}{\mu_{i+1}k_i + \mu_i k_{i+1}} \tag{3}$$

When the wave given by (1) passes through the multilayered medium, multiple reflections and transmissions occur along each layer transition. The generalized reflection coefficient includes the effect of subsurface reflections. For the interface between region i and region $i+1$, the generalized reflection coefficient $\tilde{R}_{i,i+1}$ can be written as [12]:

$$\tilde{R}_{i,i+1} = \frac{R_{i,i+1} + \tilde{R}_{i+1,i+2}e^{2jk_{i+1}(d_{i+1}-d_i)}}{1 + R_{i,i+1}\tilde{R}_{i+1,i+2}e^{2jk_{i+1}(d_{i+1}-d_i)}}, \tag{4}$$

where $R_{i,i+1}$ is the reflection coefficient given by (2) and $z = -d_i$ is the interface between region i and region $i+1$ as shown in Fig. 3. The expression forms a recursive relation that expresses $\tilde{R}_{i,i+1}$ in terms of $\tilde{R}_{i+1,i+2}$. Since $\tilde{R}_{N,N+1} = 0$, (4) can be solved recursively for $\tilde{R}_{i,i+1}$ in all regions.

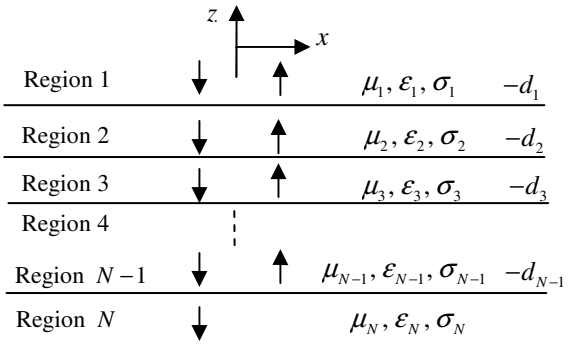

Fig. 3. Reflection and transmission in a multilayered medium. μ_i, ε_i and σ_i are the permeability, permittivity and conductivity respectively in Region *i*.

The generalized transmission coefficient $\tilde{T}_{1,N}$ can be obtained as:

$$\tilde{T}_{1,N} = \prod_{i=1}^{N-1} e^{jk_i(d_i - d_{i-1})} S_{i,i+1}, \tag{5}$$

where

$$S_{i,i+1} = \frac{T_{i,i+1}}{1 - R_{i+1,i}\tilde{R}_{i+1,i+2}e^{2jk_{i+1}(d_{i+1}-d_i)}}, \tag{6}$$

$d_0 = d_1$ and $T_{i,i+1}$ is the transmission coefficient as given by (4). Hence the down-going wave amplitude in region N at $z = -d_{N-1}$ is just $\left|\tilde{T}_{1,N}\right|$ times the down-going wave amplitude in region 1 at $z = -d_1$. $\tilde{T}_{1,N}$ follows the reciprocal property $\frac{\mu_1}{k_1}\tilde{T}_{1,N} = \frac{\mu_N}{k_N}\tilde{T}_{N,1}$.

The time-averaged power in region N at the interface $z = -d_{N-1}$ can be obtained by:

$$P_N = \frac{\left|\tilde{T}_{1,N}\right|^2 e_0^2}{2|\eta_N|}\cos\theta_N, \tag{7}$$

where η_N is the intrinsic impedance of region N, θ_N is its phase angle and e_0 is the down-going wave amplitude at $z = -d_1$.

Hence the transmission power loss is simply given by:

$$\begin{aligned} L_P(dB) &= -10\log_{10}\left(P_N \big/ P_1\right) \\ &= -10\log_{10}\left(\left|\tilde{T}_{1,N}\right|^2 \frac{|\eta_1|\cos\theta_N}{|\eta_N|\cos\theta_1}\right) \end{aligned} \tag{8}$$

IV. TRANSMISSION POWER LOSS VARIATION

The variation in the transmission power loss due to the different thicknesses of the tissues is investigated using the layered planar model and generalized transmission coefficient. In order to get an overview of the effect of the variation of the thickness of each tissue on the transmission power, the transmission power loss is first obtained by varying the thickness of one tissue at a time, while fixing the thicknesses of all the other tissues. From Table IV, in consideration of all tertiles at 923 MHz, the thickness of skin, subcutaneous fat, abdominal muscle and visceral fat varies from 1.1–1.6 mm, 11.5–28.5 mm, 8.0–16.0 mm and 11.0–104.0 mm, respectively. In this study, the thicknesses of the skin, subcutaneous fat, abdominal muscle and visceral fat are fixed at 1.4 mm, 20 mm, 12 mm and 75 mm, respectively.

Figs. 4–6 show the plot of the transmission power loss versus the thickness of visceral fat, subcutaneous fat and abdominal muscle, respectively. Due to the multiple reflections between layers, the reflected and transmitted waves can combine constructively or destructively due to the

variation in the phase. Hence, the resultant transmission power loss does not increase monotonically with the increase in tissue thickness, as seen from the plots for the visceral and subcutaneous fat at 923 MHz. Also, the effect of the visceral fat thickness variation on the power loss is the largest. The plot for skin thickness variation is not shown as its effect is negligible.

The HUGO model in Fig. 1 has around 100 mm of visceral fat thickness at the center of the belly. As the capsule endoscope travels in the small intestine, the RF propagation path from the small intestine to the belly skin surface will experience varying abdominal tissue thicknesses. Hence, the propagation path should include the visceral fat thickness that ranges from 10 mm to 100 mm. Since the effect of the visceral fat thickness on the power loss is the largest, Fig. 4 gives an indication of the transmission power loss variation of the capsule using the HUGO model. From Fig. 4, the transmission power loss variation is 8.16 dB and 4.89 dB at 403 MHz and 923 MHz, respectively.

Next, the power loss transmission for the different male subjects who are grouped according to the visceral fat thickness is considered [11]. The skin, subcutaneous fat, abdominal muscle and visceral fat thickness is varied in steps of 0.05 mm, 0.5 mm, 0.5 mm and 1 mm, respectively for the range of thicknesses shown in Table IV. Table V shows the range, mean and standard deviation of transmission power loss due to the variation in the tissue thicknesses. In general, the transmission power loss at 403 MHz is higher than that at 923 MHz. As for transmission power variation, the variation of visceral fat thickness in the high tertile group has the greatest effect on the transmission power loss at 923 MHz. On the other hand, the transmission power loss variation at 403 MHz is the largest for the visceral fat thickness in the low tertile group. At 403 MHz, the transmission power loss variation is 9 dB, 5 dB and 4.4 dB for the low, mid and high tertile group, respectively. At 923 MHz, the transmission power loss variation is 6.3 dB, 4.6 dB and 7.3 dB for low, mid and high tertile group, respectively. Across all tertiles, the transmission power loss variation is 11.1 dB (4.4−15.5 dB) at 403 MHz and 8.3 dB (6.8−15.1 dB) at 923 MHz.

It is to be noted that the investigations are more concerned with the variation in the transmission power, rather than the absolute transmission power for an ingestible radiator. Hence, a uniform plane wave is assumed without consideration of the antenna. This is sufficient to study the trend of the effect of the abdominal tissue thicknesses on electromagnetic (EM) wave propagation. However, in order to investigate the absolute transmission power for ingestible radiator, the antenna effect (coupling with the tissues) and other near-field effects have to be considered in our future study using full wave EM simulation

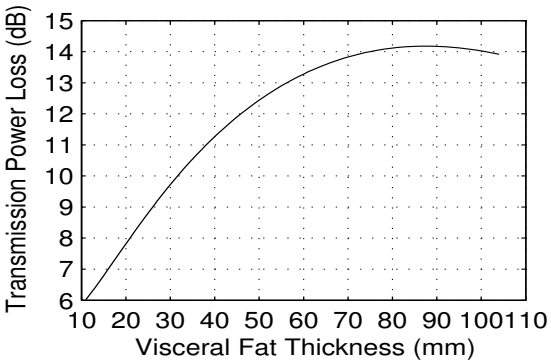

(a) 403 MHz

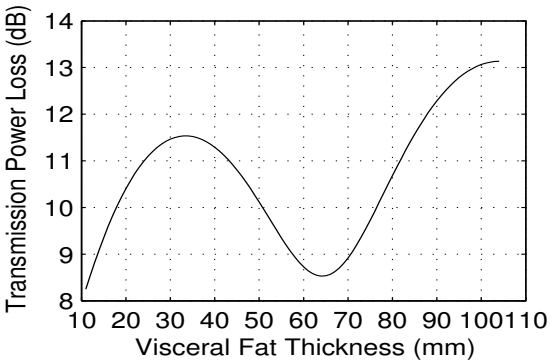

(b) 923 MHz

Fig. 4. Plot of transmission power loss (dB) versus visceral fat thickness (mm) for the layered planar tissue model at (a) 403 MHz and (b) 923 MHz. The thickness of the skin, subcutaneous fat and abdominal muscle is fixed at 1.4 mm, 20 mm and 12 mm, respectively.

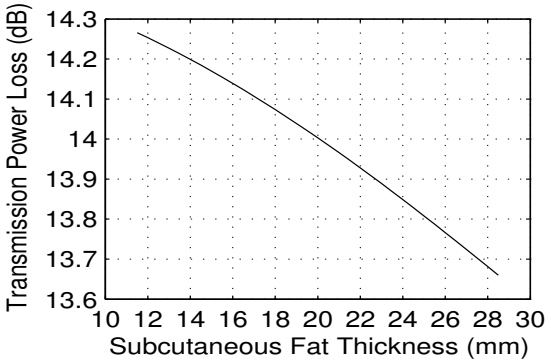

(a) 403 MHz

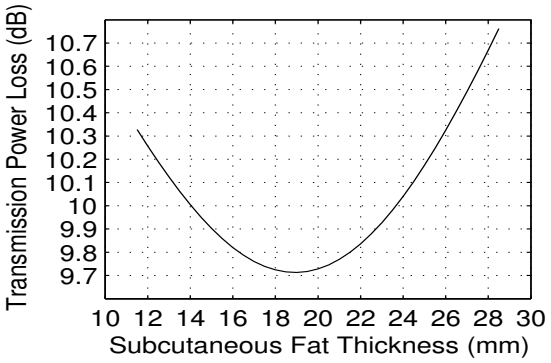

(b) 923 MHz

Fig. 5. Plot of transmission power loss (dB) versus subcutaneous fat thickness (mm) for the layered planar tissue model at (a) 403 MHz and (b) 923 MHz. The thickness of the skin, abdominal muscle and visceral fat is fixed at 1.4 mm, 12 mm and 75 mm, respectively.

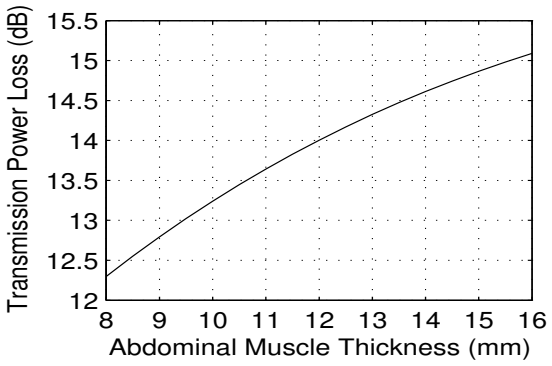

(a) 403 MHz

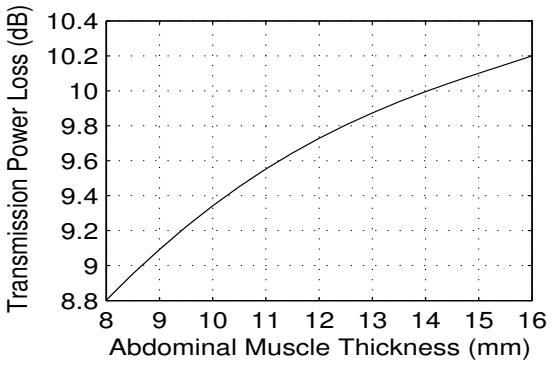

(b) 923 MHz

Fig. 6. Plot of transmission power loss (dB) versus abdominal muscle thickness (mm) for the layered planar tissue model at (a) 403 MHz and (b) 923 MHz. The thickness of the skin, subcutaneous fat and visceral fat is fixed at 1.4 mm, 20 mm and 75 mm, respectively.

TABLE V
TRANSMISSION POWER LOSS

Frequency	Transmission power loss (dB)		
	Low tertile	Mid tertile	High tertile
403 MHz	4.4 – 13.4 (9.0, 2.0)	9.6 – 14.6 (12.3, 1.1)	11.1 – 15.5 (13.8, 0.9)
923 MHz	6.8 – 13.1 (10.9, 1.1)	8.3 – 12.9 (10.2, 0.8)	7.8 – 15.1 (11.0, 1.8)

* values in the brackets represent (mean, standard deviation)

V. Discussion

Capsule endoscopy technology has to advance from offering only visual diagnosis of the GI tract to include biopsy and other therapeutic functions. In order to achieve multi-functionality, one of the major challenges lies in the research to provide a longer lasting power supply. This can be approached in two ways: (a) to improve on the power source, i.e. better batteries or provide external source of power by induction, and (b) to improve on the power management of the modules in the capsule so as to reduce the overall power consumption. The results of the RF transmission power variation in this paper can be used for the latter approach, specifically for the design of the wireless communications module of the capsule endoscope.

The wireless communications module is typically designed to ensure that the link budget is satisfied. As shown in this study, the transmission power loss variation indicates that the best and worst link in the human abdominal region can differ by up to 10 dB when different human subjects are considered. Even for an individual subject, the variation can be up to 8 dB as the capsule travels through different parts of the small intestine. The results also show that the transmission power loss variation does not follow a simple relationship with the body size variation. This is due to the complex interaction between multiple reflections among the different tissue boundaries. This implies that an adaptive RF transmit power scheme can be implemented to conserve power consumption. An adjustable pre-set transmit power level that is based on the body size of the patient before the capsule is swallowed will not be feasible as any prediction based on body size will most likely be inaccurate, as can be observed from Table V. The range of loss for low and high tertile is comparable for 923 MHz. Hence, the wireless communications module has to monitor the link and adjust the transmit power adaptively during operation.

Lastly, the comparison of the transmission power loss at 403 MHz and 923 MHz shows that the lower frequency generally results in a higher transmission loss, which is due to the more significant transition loss as the EM waves propagate across the different tissue layers. In the case of capsule endoscopy, the antenna inside the capsule needs to be small. Hence, the antenna with size limitation will have higher radiation efficiency at a higher operating frequency. In consideration of the antenna efficiency and transmission power loss, the frequency of 923 MHz may be more appropriate than 403 MHz for wireless capsule endoscopy.

VI. Conclusion

The variation in transmission power loss due to the thicknesses of the different tissues has been investigated using a layered planar tissue model of skin, subcutaneous fat, abdominal muscle, visceral fat and small intestine. Calculations have shown that the range of the thicknesses of these tissues (esp. visceral fat) can result in significant variation of the transmission power loss. This implies that different levels of RF transmit power can be used for different human subjects and capsule positions. An adaptive RF transmit power scheme can be implemented to conserve power. For further investigations, simulations and experiment will be conducted with the capsule and external antennas.

References

[1] C. McCaffrey, O. Chevalerias, C. O'Mathuna, and K. Twomey, "Swallowable-Capsule Technology," *IEEE Pervasive Computing*, vol. 7, no. 1, pp. 23 – 29, 2008.

[2] A. Moglia, A. Menciassi, M. O. Schurr, and P. Dario, "Wireless capsule endoscopy: from diagnostic devices to multipurpose robotic systems," *Biomedical Microdevices,* vol. 9, no. 2, pp. 235 - 243, Apr. 2007.

[3] M, Q.-H. Meng, T. Mei, J. Pu, C. Hu, X. Wang, and Y. Chan, "Wireless robotic capsule endoscopy: State-of-the-art and challenges," *World Congress on Intelligent Control and Automation, WCICA 2004*, vol. 6, pp. 5561 – 5565, June 2004.

[4] A. Moglia, A. Menciassi, P. Dario, and A. Cuschieri, "Capsule endoscopy: progress update and challenges ahead," *Nature Reviews Gastroenterology and Hepatology*, vol. 6, pp. 353-361, June 2009.

[5] W. G. Scanlon, J. B. Burns, and N. E. Evans, "Radiowave propagation from a tissue-implanted source at 418 MHz and 916.5 MHz," *IEEE Trans. Biomedical Engineering*, vol. 47, no. 4, pp. 527 – 534, Apr. 2000.

[6] L. C. Chirwa, P. A. Hammond, S. Roy, and D. R. S. Cumming, "Electromagnetic radiation from ingested sources in the human intestine between 150 MHz and 1.2 GHz," *IEEE Trans. Biomedical Engineering*, vol. 50, no. 4, pp. 484 – 492, Apr. 2003.

[7] A. Alomainy and Y. Hao, "Modeling and characterization of biotelemetric radio channel from ingested implants considering organ contents," *IEEE Trans. Antennas and Propagation,* vol. 57, no. 4, pp. 99 – 1005, Apr. 2009.

[8] A. Christ, A. Klingenbock, T. Samaras, C. Goiceanu, and N. Kuster, "The dependence of electromagnetic far-field absorption on body tissue composition in the frequency range from 300 MHz to 6 GHz," *IEEE Trans. Microwave Theory and Techniques*, vol. 54, no. 5, pp. 2188 – 2195, May 2006.

[9] A. Christ, T. Samaras, A. Klingenbock, and N. Kuster, "Characterization of the electromagnetic near-field absorption in layered biological tissue in the frequency range from 30 MHz to 6000 MHz," *Phys. Med. Biol.*, vol. 51, no. 19, pp. 4951 – 4965, Sep. 2006.

[10] A. Sani, A. Alomainy, and Y. Hao, "Numerical characterization and link budget evaluation of wireless implants considering different digital human phantoms," *IEEE Trans. on Microwave Theory and Techniques*, vol. 57, no. 10, pp. 2605 – 2613, Oct. 2009.

[11] S. K. Kim, et. al., "Visceral fat thickness measured by ultrasonography can estimate not only visceral obesity but also risks of cardiovascular and metabolic diseases," *American Journal of Clinical Nutrition*, vol. 79, no. 4, pp. 593-599, 2004.

[12] W. C. Chew, *Waves and fields in inhomogeneous media*, Van Nostrand Renhold, 1990.

[13] M. J. Ackerman, "The visible human project," *Proc. IEEE*, vol. 86, no. 3, pp. 504 – 511, Mar. 1988.

[14] S. Gabriel, R. W. Lau, and C. Gabriel: "The dielectric properties of biological tissues: III. Parametric models for the dielectric spectrum of tissues," *Phys. Med. Biol.*, vol. 41, pp. 2271-2293, 1996.

[15] Y. Lee and K. Hwang, "Skin thickness of Korean adults," *Surgical and Radiologic Anatomy*, vol. 24, no. 3 – 4, pp. 183 – 189, 2002.

[16] H. Kanehisa, et. al., "Influences of age and sex on abdominal muscle and subcutaneous fat thickness," *Euro. J. Appl. Physiol.*, vol. 91, no. 5 – 6, pp. 534 – 537, May 2004.